Received: 12 July 2019 | Revised: 3 September 2019 | Accepted: 4 September 2019

DOI: 10.1111/jace.16791

Journal of the American Ceramic Society

ORIGINAL ARTICLE

Phase evolution and microwave dielectric properties of novel $LiAl_{5-x}Zn_xO_{8-0.5x}$-based ($0 \leq x \leq 0.5$) ceramics

Xue-Kai Lan[1,2] | **Jie Li**[1,2] | **Jia-Pu Li**[1] | **Fei Wang**[1,2] | **Wen-Zhong Lu**[1,2] | **Xiao-Chuan Wang**[1,2] | **Wen Lei**[1,2]

[1]School of Optical and Electronic Information, Huazhong University of Science and Technology, Wuhan, P. R. China

[2]Key Lab of Functional Materials for Electronic Information (B), Ministry of Education, Wuhan, P. R. China

Correspondence
Wen Lei, School of Optical and Electronic Information, Huazhong University of Science and Technology, Wuhan 430074, P. R. China.
Email: wenlei@mail.hust.edu.cn

Funding information
National Natural Science Foundation of China, Grant/Award Number: 51772107, 51572093 and 61771215; Major Technological Innovation Projects in Hubei Province, Grant/Award Number: 2018AAA039; Equipment Development Department, Grant/Award Number: 1807WM0004

Abstract

Novel $LiAl_{5-x}Zn_xO_{8-0.5x}$ microwave dielectric ceramics were synthesized through a solid-state reaction route. Phase evolution of $LiAl_{5-x}Zn_xO_{8-0.5x}$ was determined by XRD analysis. The XRD results indicated that the phase compositions had a $P4_332$ space group when $0 \leq x \leq 0.2$ and a spinel structure when $0.3 \leq x \leq 0.5$. The dielectric constant (ε_r) of this series' solid solutions decreased with the increase in Zn doping content, which was in good agreement with the Clausius-Mossotti relation. Oxygen vacancy and the decreased degree of order degraded the quality factor ($Q \times f$) of the two structures. The deterioration in quality factor was further verified by impedance spectroscopy. The temperature coefficient of the resonant frequency (τ_f) decreased with the increase in x and was correlated with the unit cell volume. Finally, $CaTiO_3$ was used as a compensation material to obtain a near-zero τ_f of the $LiAl_5O_8$ ceramic.

KEYWORDS

dielectric materials/properties, electroceramics, microstructure, microwaves

1 | INTRODUCTION

The development of wireless communication systems requires electronic devices and substrates to have high frequency applications, miniaturization capabilities, and low-loss properties.[1–3] Dielectric ceramics with low ε_r and high $Q \times f$ are important materials for resonators, filters, and other key components from terrestrial to satellite communication systems, including the Internet of Thing (IoT), RFID, DBS TV, GPS, etc. Thus, these materials are gaining attention for academic and commercial purposes.[4–6]

Various microwave dielectric ceramic systems, such as Bi_2O_3–TiO_2–V_2O_5, (Sr, Ca)TiO_3–$LnAlO_3$ (Ln = La, Nd, Sm), and BaO–Ln_2O_3–TiO_2,[7,8] with high $Q \times f$ have attracted considerable research attention. Li_2O–Al_2O_3 ceramic systems, including Li_5AlO_4, $LiAlO_2$, and $LiAl_5O_8$, have seldom been studied for the application as microwave dielectric materials. In the past few years, we have investigated the $LiAlO_2$ ceramics for microwave dielectric application.[9] On the other hand, the use of $LiAl_5O_8$ material as microwave dielectric ceramics have not been reported before. The $LiAl_5O_8$ compound with $P4_332$ space group is a cubic ordered structure of four formula units in the unit cell $Al_8^{IV}(Li_4Al_{12})^{VI}O_{32}$, and in the octahedral (o) sites there exist 1:3 ordering of Li: Al.[10] A previous solid-state magic angle spinning nuclear magnetic resonance spectrum analysis on the $LiAl_5O_8$ compound showed that the substitution of Zn^{2+} and Mg^{2+} ions does not affect the distribution in octahedral sites of all the Li^+ ions. However, Al^{3+} ions in octahedral (o) and tetrahedral (t) sites are affected and

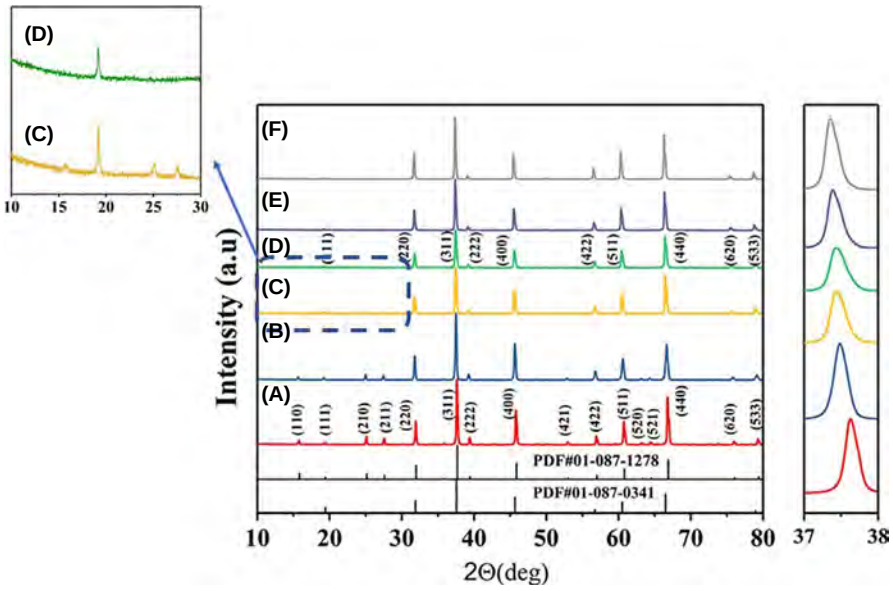

FIGURE 1 XRD patterns of $LiAl_{5-x}Zn_xO_{8-0.5x}$ ($0 \le x \le 0.5$) ceramics at 1600°C for 6 h: (A) $x = 0$; (B) $x = 0.1$; (C) $x = 0.2$; (D) $x = 0.3$, (E) $x = 0.4$, (F) $x = 0.5$

redistributed. An infrared spectrum analysis of Zn^{2+}-doped $LiAl_5O_8$ ceramic indicated that increased Zn^{2+} substitution content can result in an increasingly disordered form.[11] The substitution of Zn^{2+} and Mg^{2+} ions for Al^{3+} ions also induces the phase transition of the $LiAl_5O_8$ compound.

In this work, $LiAl_{5-x}Zn_xO_{8-0.5x}$ materials were sintered through conventional solid-state method. Then the effects of Zn^{2+} ion substitute to the Al^{3+} ion sites on the properties of the $LiAl_5O_8$ compound were investigated. The relationship among the crystal structure, phase transition, and microwave dielectric properties of the $LiAl_{5-x}Zn_xO_{8-0.5x}$ ceramics was studied.

2 | EXPERIMENTAL PROCEDURE

$LiAl_{5-x}Zn_xO_{8-0.5x}$ materials were prepared by the solid-state reaction method. Stoichiometric Li_2CO_3, ZnO, and Al_2O_3 reagents were mixed using alcohol by ball milling. The dried powder was calcined in a furnace for 900°C. Then, the calcined powder was milled again in the same manner as before. The powder was pressed in a disk and sintered in air for 1600°C. A $CaTiO_3$ commercial reagent with a ratio of $(1 - y)$ $LiAl_5O_8 + y$ $CaTiO_3$ ($y = 0.02-0.08$) was added to the calcined $LiAl_5O_8$ powder in the same manner as discussed above and then sintered at a furnace for 1500°C.

The microstructure of thermal etching samples was examined by scanning electron microscopy (SEM). The crystal structure of $LiAl_{5-x}Zn_xO_{8-0.5x}$ ($0 \le x \le 0.5$) ceramics was measured using X-ray diffractometer (XRD). Then using GSAS software[12] to refine the XRD data and obtain the lattice parameters.

The microwave dielectric properties of the $LiAl_{5-x}Zn_xO_{8-0.5x}$ ceramics were recorded in a microwave network analyzer using the Hakki and Coleman methods.[13] Furthermore, the τ_f value was calculated using

$$\tau_f = \frac{1}{f(T_0)} \frac{[f(T_1) - f(T_0)]}{T_1 - T_0}, \quad (1)$$

$f(T_0)$ and $f(T_1)$ represent the resonant frequency at T_0 (30°C) and T_1 (80°C). An impedance analyzer was used to analyze the impedance spectroscopy of the samples in the frequency between 100 Hz and 10 MHz.

3 | RESULTS AND DISCUSSION

Figure 1 shows the XRD profiles of $LiAl_{5-x}Zn_xO_{8-0.5x}$ ceramics. As shown in the figure, the intensity of a few low-angle X-ray peaks, such as (110), (210), and (211), gradually weakens and then disappears at $x = 0.3$ with the increased Zn content. When $x \le 0.2$, the phase belongs to the $P4_332$ space group. When $0.3 \le x \le 0.5$, the series of materials have the Fd-3m space group of a spinel structure. Thus, the different Zn content substitutions on the Al site can lead to phase transition in the $LiAl_5O_8$ material, which occurs at approximately $x = 0.3$.

The influence of Zn substitution of these samples on the lattice parameters was obtained using Rietveld refinement method. The refinement result of $LiAl_{5-x}Zn_xO_{8-0.5x}$ ($x = 0$, 0.3) ceramics is shown in Figure 2 and Table 1. The lattice parameters and relative density of the samples are shown in Table 2. The table reveals that the lattice parameters increase as the increased Zn content. Moreover, the strongest peak (311) shifts to the lower 2θ angle with the increase in x shown in Figure 1. Bragg's law ($2d\sin\theta = n\lambda$) posits that this phenomenon also indicates an increase in lattice parameters. According to the literature,[14] the radii of Zn^{2+} and Al^{3+} are

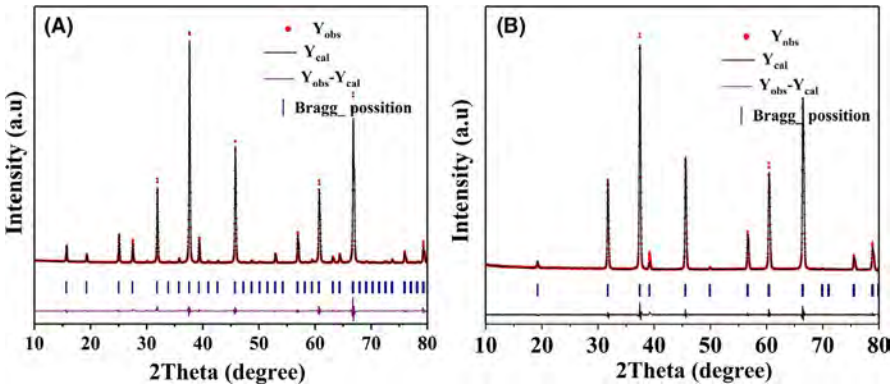

FIGURE 2 Rietveld refinement of (A) $LiAl_{5-x}Zn_xO_{8-0.5x}$ ($x = 0$) and (B) $LiAl_{5-x}Zn_xO_{8-0.5x}$ ($x = 0.3$) ceramic sintered at 1600°C for 6 h

TABLE 1 Refined structural parameters of $LiAl_{5-x}Zn_xO_{8-0.5x}$ ceramic. The subscript 1 represent for $x = 0$, and subscript 2 represent for $x = 0.3$

Atom	*x*	*y*	*z*	Fraction	R_p	R_{wp}	χ^2
$Li1_1$	0.625	0.625	0.625	1.00	0.061	0.087	4.931
$Li2_1$	0.07352	0.17648	0.125	1.00			
$Al1_1$	−0.00174	-0.00174	-0.00174	1.00			
$Al2_1$	0.625	0.625	0.625	1.00			
$Al3_1$	0.368008	-0.11801	0.125	1.00			
$O1_1$	0.115794	0.130097	0.130097	1.00			
$O2_1$	0.386521	0.386521	0.386521	1.00			
Li_2	0.5	0.5	0.5	1.00	0.066	0.093	5.101
$Al1_2$	0.125	0.125	0.125	0.94			
$Al2_2$	0.5	0.5	0.5	0.94			
$Zn1_2$	0.125	0.125	0.125	0.06			
$Zn2_2$	0.5	0.5	0.5	0.06			
O_2	0.24895	0.24895	0.24895	1.00			

TABLE 2 Lattice parameters and relative densities of $LiAl_{5-x}Zn_xO_{8-0.5x}$ ceramics sintered at 1600°C for 6 h in air

x	Lattice parameter *a* (Å)	Unit cell volume (Å^3)	Calculated density (g/cm^3)	Relative density (%)
0	7.908	494.538	3.624	92.3
0.1	7.914	495.665	3.657	95.5
0.2	7.938	500.188	3.664	95.7
0.3	7.949	502.270	3.689	96.2
0.4	7.961	504.548	3.713	96.3
0.5	7.968	505.881	3.743	96.1

0.74 and 0.535 Å, respectively. Therefore, the substitution of a Zn^{2+} ion (large radius) for an Al^{3+} ion (small radius) can enlarge the lattice parameters in the $LiAl_{5-x}Zn_xO_{8-0.5x}$ ceramics. All the samples, except for $x = 0$, possess a relative density of more than 95%. This finding suggests that the Zn^{2+} substitution improves the density and that the compositions are compact when sintered at 1600°C.

The thermally etched morphology of the $LiAl_{5-x}Zn_xO_{8-0.5x}$ ($0 \le x \le 0.5$) materials is shown in Figure 3. All the samples can be sintered well at 1600°C. It can be seen that there are very few pores in composition of $x = 0$. However, with the increase in Zn content, the pores are gradually disappeared and almost no porosity in the compacted morphology of the samples could be obtained finally. This result further confirms the high relative density in Table 2. Of all the samples, the grain sizes are below 2 μm, and the Zn doping content can slightly affect the grain size. The grain size of the samples gradually increases with the increased Zn content.

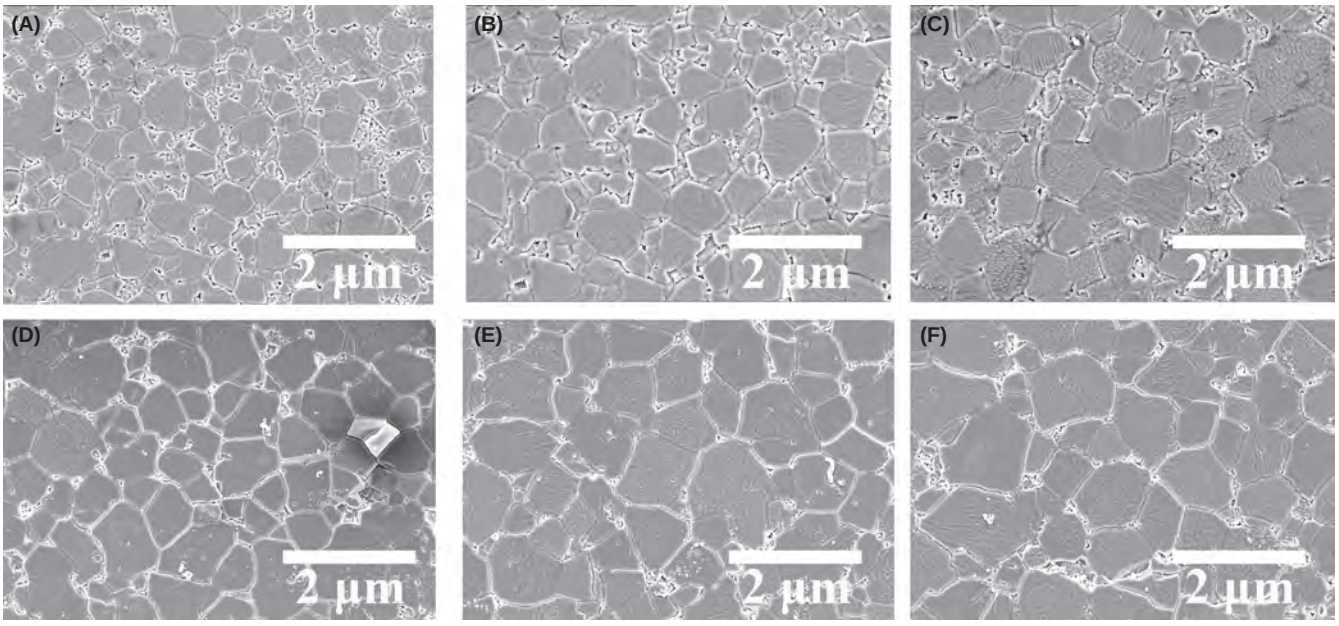

FIGURE 3 SEM micrograph of $LiAl_{5-x}Zn_xO_{8-0.5x}$ ($0 \le x \le 0.5$) ceramics sintered at 1600°C: (A) $x = 0$; (B) $x = 0.1$; (C) $x = 0.2$; (D) $x = 0.3$, (E) $x = 0.4$, (F) $x = 0.5$

The microwave dielectric properties of the $LiAl_{5-x}Zn_xO_{8-0.5x}$ ceramics are shown in Figure 4. ε_r gradually decreases from 8.43 to 8.04 with the increase in x from 0 to 0.5. Studies have shown that ε_r generally depends on porosity, microstructure, polarizability, and the secondary phase.[15] The corrected dielectric constant values (ε_{corr}) were used in the following equation[16]:

$$\varepsilon_r = \varepsilon_{corr}\left(1 - \frac{3P\left(\varepsilon_{corr}-1\right)}{2\varepsilon_{corr}+1}\right). \quad (2)$$

As shown in Table 3, the corrected porosity values (ε_{corr}) have the identical tendency of the measured ones, which is the same as the previous literature.[17] Shannon[18] reported that the total dielectric polarizability (α_D^T) of complex materials can be decomposed into ion polarizabilities (α_D). For the $LiAl_{5-x}Zn_xO_{8-0.5x}$ series ceramics, the dielectric polarizability (α_D^T) of the can be calculated as

$$\alpha_D^T(LiAl_{5-x}Zn_xO_{8-0.5x}) = \alpha(Li^+) + (5-x)\alpha(Al^{3+}) + x\alpha(Zn^{2+}) + (8-0.5x)\alpha(O^{2-}). \quad (3)$$

According to the Clausius-Mossotti relation, ε_c can be calculated as

$$\varepsilon_c = \frac{1+2b\alpha_D^T/V_m}{1-b\alpha_D^T/V_m}, \quad (4)$$

where $b = 4\pi/3$, and V_m is the mole volume of the crystal and can be obtained through the Rietveld refinement value. The ionic-polarizability values of Li^+, Al^{3+}, Zn^{2+}, and O^{2-} are 1.20, 0.78, 2.09, and 2.00 Å^3, respectively.[18] As shown

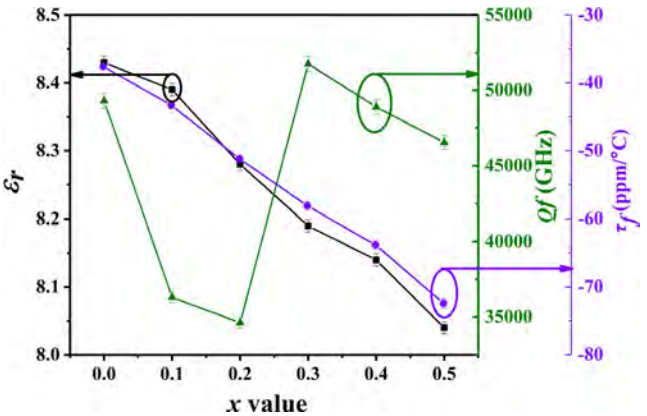

FIGURE 4 The ε_r, $Q \times f$ and τ_f values of the $LiAl_{5-x}Zn_xO_{8-0.5x}$ ($0 \le x \le 0.5$) ceramics as a function of x value

TABLE 3 The calculated dielectric polarizability (α_D^T), corrected dielectric constant ε_{corr}, and calculated dielectric constant ε_c value of $LiAl_{5-x}Zn_xO_{8-0.5x}$ ($0 \le x \le 0.5$) ceramics

x	α_D^T (Å^3)	V_m (Å^3)	ε_r	ε_{corr}	ε_c
0	84.400	494.538	8.43	9.34	8.51
0.1	84.524	495.665	8.39	9.00	8.49
0.2	84.648	500.188	8.28	8.76	8.29
0.3	84.772	502.270	8.19	8.64	8.23
0.4	84.896	504.548	8.14	8.54	8.15
0.5	85.020	505.881	8.04	8.53	8.12

in Table 3, the calculated dielectric constant (ε_c) also has the same tendency as the observed ε_r.

Figure 4 shows the $Q \times f$ value of the $LiAl_{5-x}Zn_xO_{8-0.5x}$ ceramics. For $P4_332$ space group structure, that is, $0 \le x \le 0.2$, the $Q \times f$ value decreases from 49 300 to 36 300 GHz. For the spinel structure, that is, $0.3 \le x \le 0.5$, $Q \times f$ decreases from 51 700 to 46 500 GHz. In general, lattice defects, porosity, disorder of ions, and band gap considerably influence the $Q \times f$ value. Given that we utilized the bivalent Zn^{2+} ion as substitute for the trivalent Al^{3+} ion, oxygen vacancy will be induced in the compound. This condition causes the deterioration of the $Q \times f$ value for the two space group materials. The decreased degree of order can also lead to the degradation of the $Q \times f$ value. As reported by Ishimaru et al[19] that the XRD pattern of the ordered spinel shows high intensity of all odd reflection peaks and low intensity of all even reflection peaks. Therefore, an order-disorder phase transition could be deduced by comparing the intensity of odd and even reflection peaks. The order parameter (ΔI) of the spinel structure can be calculated as[20]

$$\Delta I = I_o / \left(I_o + I_e\right), \tag{5}$$

where I_o and I_e refer to the intensity of odd and even reflection peaks, respectively. Using Formula (4) for the order parameter, we listed the values of ΔI in Table 4 for the spinel structure with $0.3 \le x \le 0.5$, where I_o and I_e are the (311) and (400) peaks for the samples, respectively. The finding shows that the order parameters decrease with the increased Zn doping value. Therefore, for the spinel structure of the $LiAl_{5-x}Zn_xO_{8-0.5x}$ ($0.3 \le x \le 0.5$) ceramics, the degree of order decreases with the increase in x. This situation results in the deterioration of $Q \times f$.

Figure 5 shows the measured impedance spectroscopy data of $LiAl_{5-x}Zn_xO_{8-0.5x}$ ceramics. Bulk conductivity (σ_b) value was obtained using the equivalent circuit fitting method through the original impedance data. Every temperature response in the Figure 5 was fitted using parallel R-CPE

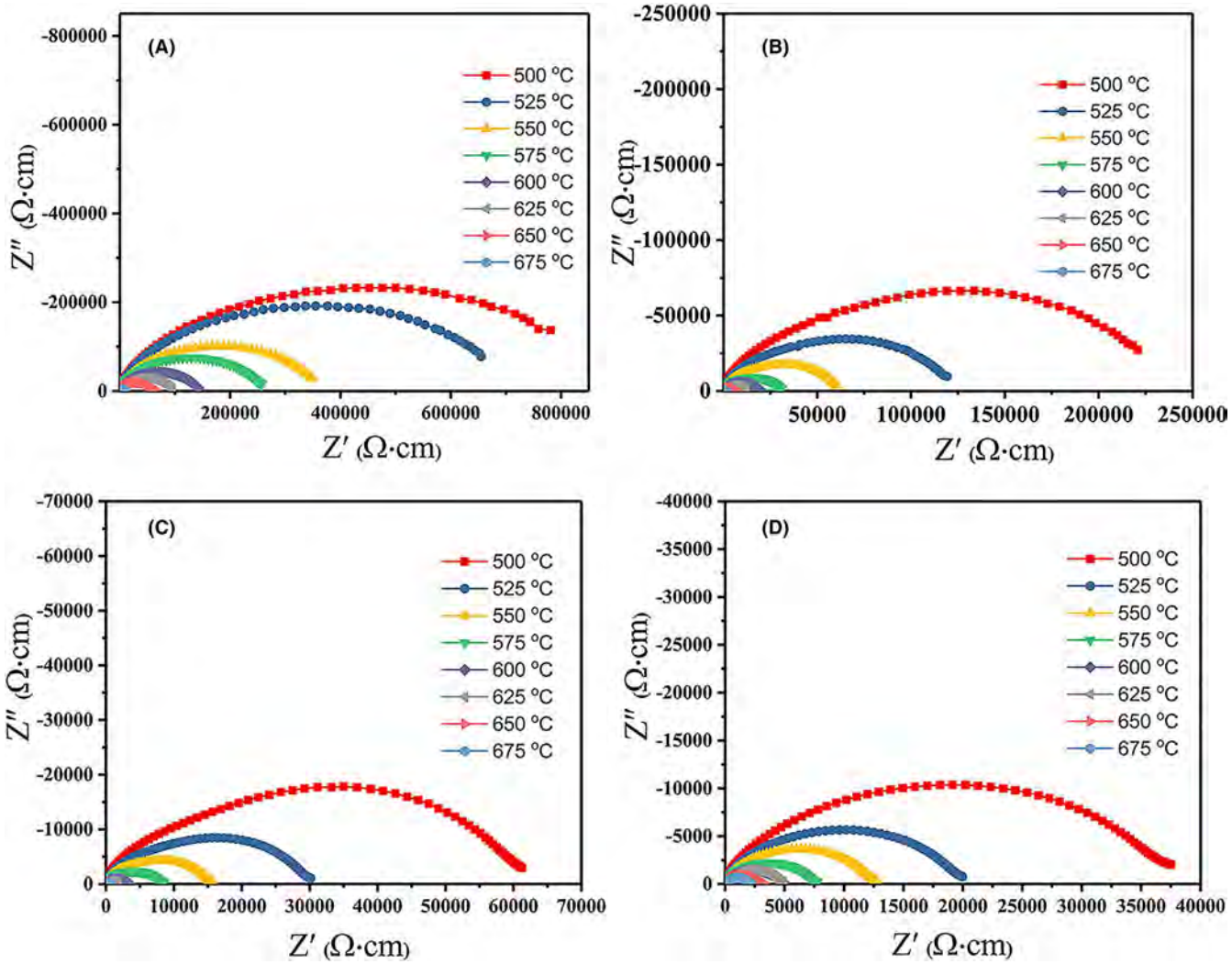

FIGURE 5 Original impedance spectroscopy data of $LiAl_{5-x}Zn_xO_{8-0.5x}$ ceramics: (A) $x = 0$; (B) $x = 0.1$; (C) $x = 0.3$, (D) $x = 0.4$

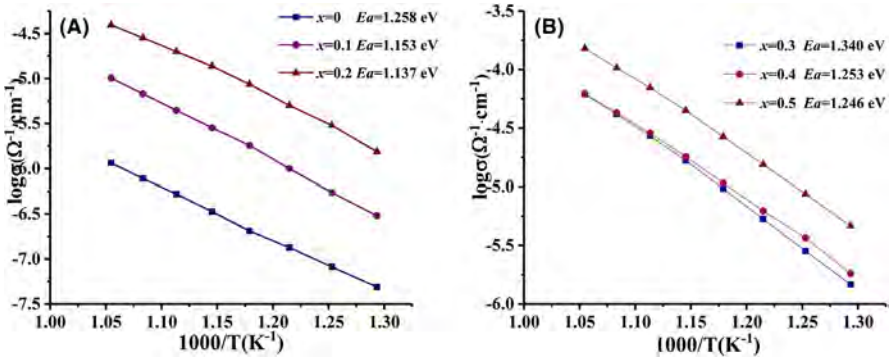

FIGURE 6 Arrhenius fitting plot from the temperature dependence of the bulk conductivity for $LiAl_{5-x}Zn_xO_{8-0.5x}$ ceramics: (A) $0 \le x \le 0.2$; (B) $0.3 \le x \le 0.5$

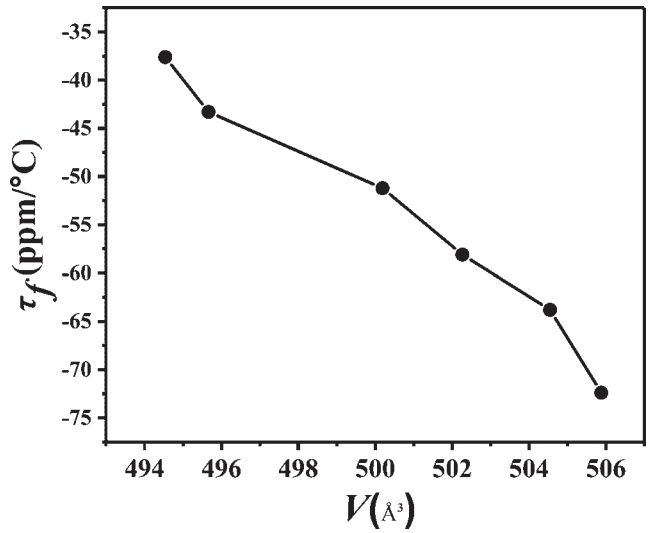

FIGURE 7 Variation of τ_f value as a function of unit-cell volume V

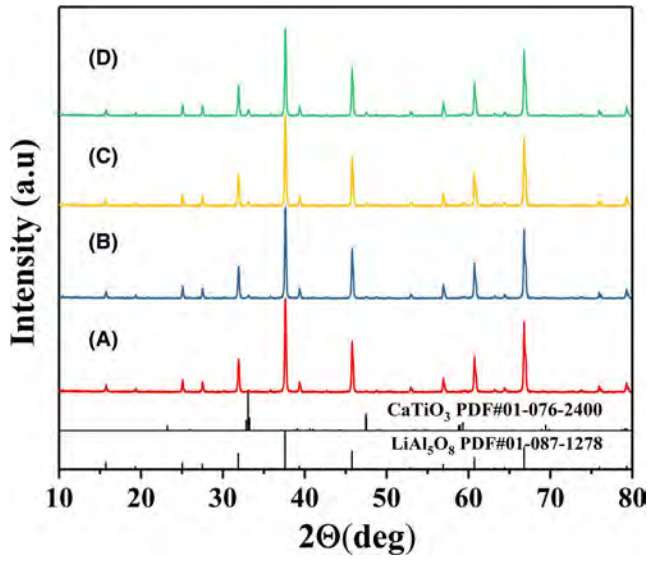

FIGURE 8 XRD patterns of the $(1-y)\ LiAl_5O_8 + y\ CaTiO_3$ ($y = 0.02$-0.08) ceramics sintered at 1500°C in air for 6 h: (A) $x = 0.02$; (B) $x = 0.04$; (C) $x = 0.06$; (D) $x = 0.08$

elements. Then, the obtained bulk resistance R was converted to conductivity using Formula (6),

$$\sigma_b = \frac{1}{R_b}\frac{4t}{\pi D^2}, \tag{6}$$

where t represents thickness and D represents diameter. The Arrhenius fit of the σ_b for $LiAl_{5-x}Zn_xO_{8-0.5x}$ ceramics of $0 \le x \le 0.2$ and $0.3 \le x \le 0.5$ are exhibited in Figure 6. As x increases from 0 to 0.2, the calculated activation energy (E_a) has a decreasing tendency from 1.258 to 1.137 eV. Meanwhile, E_a decreases from 1.340 to 1.264 eV when x changes from 0.3 to 0.5. On the basis of the approximation of the intrinsic band gap, $E_g \approx 2E_a$,[21–23] the conductivity was deduced with the increase in x from 0 to 0.2 and 0.3 to 0.5. Thus, the samples at $x = 0$ and 0.3 have the highest quality factor for the different lattice structures, that is, $0 \le x \le 0.2$ and $0.3 \le x \le 0.5$, respectively, of the $LiAl_{5-x}Zn_xO_{8-0.5x}$ ceramics.

As x increases from 0 to 0.5, τ_f increases from −38 ppm/°C to −72 ppm/°C in the negative direction, as shown in Figure 4. Previous studies[24–26] indicated that the τ_f value is proportional to the relative magnitude of the cell volume of the compound. Figure 7 shows that τ_f decreases with the increase in unit cell volume, which is consistent with previous results.

TABLE 4 Order parameter ΔI as a function of x value

x	I_o (311)	I_e (400)	ΔI
0.3	100	39.9	0.715
0.4	100	42.6	0.701
0.5	100	46.3	0.684

TABLE 5 Microwave dielectric properties of $(1-y)$ $LiAl_5O_8 + y\ CaTiO_3$ ($y = 0.02$-0.08) ceramics sintered at 1500°C for 6 h

y Value	ε_r	$Q \times f$ (GHz)	τ_f (ppm/°C)
0.02	8.66	36 800	−25
0.04	8.99	26 400	−13
0.06	9.33	21 300	−5
0.08	9.76	15 200	12

For the application of microwave dielectric ceramics, a near-zero τ_f value is needed.[27] In general, some positive τ_f value materials, such as TiO_2 and $CaTiO_3$, are utilized as compensation materials for negative τ_f value materials to acquire a near-zero τ_f value. The XRD profile of $(1-y)$ $LiAl_5O_8 + y$ $CaTiO_3$ ($y = 0.02$-0.08) ceramics exhibit only two phases of $LiAl_5O_8$ and $CaTiO_3$ shown in Figure 8. The intensity of main peak of $CaTiO_3$ phase at about 33° of the XRD pattern is strengthen with the increase in y. This condition indicates an increased $CaTiO_3$ content. Table 5 lists the ε_r, $Q \times f$, and τ_f value of $(1-y)$ $LiAl_5O_8 + y$ $CaTiO_3$ ($y = 0.02$-0.08) ceramics. As shown from this table, ε_r monotonously increases from 8.66 to 9.76, while $Q \times f$ decreases significantly from 36 800 to 15 200 GHz. On the other hand, τ_f value varies from −25 to 12 ppm/°C, which means that by adjusting the content of $CaTiO_3$ a near zero τ_f value can be achieved. In this case, the best τ_f value can be achieved at $y = 0.06$ with −5 ppm/°C. The microwave dielectric properties of two phase materials generally obey the mixing rules:[28,29]

$$\ln \varepsilon_r = v_1 \ln \varepsilon_1 + v_2 \ln \varepsilon_2, \tag{7}$$

$$Q^{-1} = v_1 Q_1^{-1} + v_2 Q_2^{-1}, \tag{8}$$

$$\tau_f = v_1 \tau_{f1} + v_2 \tau_{f2}, \tag{9}$$

$$v_1 + v_2 = 1, \tag{10}$$

where v_1 and v_2 represent the volume fraction of the components. According previous study of $CaTiO_3$ ceramic, it has the trait of high ε_r, low $Q \times f$, and large τ_f value.[30,31] This character of the $CaTiO_3$ ceramic increases ε_r and τ_f and decreases the $Q \times f$ of $(1-y)$ $LiAl_5O_8 + y$ $CaTiO_3$ ($y = 0.02$-0.08) ceramics with the increase in y (Table 5).

4 | CONCLUSIONS

A series of $LiAl_{5-x}Zn_xO_{8-0.5x}$ ($0 \le x \le 0.5$) microwave dielectric ceramics with good crystallinity of uniform crystal grains and high relative density were investigated. The phase transition of this series solid solutions occurred at approximately $x = 0.3$. A pure phase with a cubic structure ($P4_332$) was formed with the increase in x from 0 to 0.2, whereas a spinel structure (Fd-3m) was obtained with the increase in x from 0.3 to 0.5. The lattice parameter (a) monotonously increased from 7.908 to 7.968 Å with the increase in x from 0 to 0.5 through Rietveld refinement. An observed ε_r very close to the calculated ε_c was obtained through the Clausius-Mossotti relation, and it monotonously decreased from 8.43 to 8.04 with the increase in x from 0 to 0.5. For the samples of the $P4_332$ space group structure, $Q \times f$ dropped from 49 300 to 36 300 GHz. For the spinel structure, $Q \times f$ dropped from 51 700 to 46 500 GHz. The defect of oxygen ion and the decreased degree of order caused this reduction in $Q \times f$. τ_f decreased from −38 ppm/°C to −72 ppm/°C in the negative direction with the increase in x from 0 to 0.5. Moreover, τ_f was correlated with the unit cell volume of $LiAl_{5-x}Zn_xO_{8-0.5x}$ for the $P4_332$ and Fd-3m space group structures. The $CaTiO_3$ material with a positive τ_f was used to compensate for the $LiAl_5O_8$ material with a negative τ_f to obtain a temperature stable material for practical applications. The $(1-y)$ $LiAl_5O_8 + y$ $CaTiO_3$ ceramic showed a near-zero τ_f when $y = 0.06$ and had microwave dielectric properties of $\varepsilon_r = 9.33$, $Q \times f = 21\,300$ GHz, and $\tau_f = -5$ ppm/°C.

ACKNOWLEDGMENTS

This work was supported by the NSFC (No. 51772107, 51572093 and 61771215), the Major Technological Innovation Projects in Hubei Province (2018AAA039), and the Equipment Development Department (1807WM0004). The authors are grateful to the Analytical and Testing Center, Huazhong University of Science and Technology.

ORCID

Wen Lei https://orcid.org/0000-0003-1164-0233

REFERENCES

1. Pang LX, Zhou D. Modification of $NdNbO_4$ microwave dielectric ceramic by Bi substitutions. J Am Ceram Soc. 2019;102(5):2278–82.
2. Lai Y, Su H, Wang G, Tang X, Huang X, Liang X, et al. Low temperature sintering of microwave ceramics with high $Q \times f$ values through LiF addition. J Am Ceram Soc. 2019;102(4):1893–903.
3. Liu B, Huang YH, Song KX, Li L, Chen XM. Structural evolution and microwave dielectric properties in $Sr_2(Ti_{1-x}Sn_x)O_4$ ceramics. J Eur Ceram Soc. 2018;38(11):3833–9.
4. Li HT, Li Q, Yan YF, Xu RH. Effect of ZnO-doping on sinterability and microwave dielectric property of $Ca_{0.25}(Li_{0.43}Sm_{0.57})_{0.75}TiO_3$ ceramics. J Inorg Mater. 2015;30(4):369–73.
5. Wang K, Zhou H, Liu X, Sun W, Chen X, Ruan H. A lithium aluminium borate composite microwave dielectric ceramic with low permittivity, near-zero shrinkage, and low sintering temperature. J Eur Ceram Soc. 2019;39(4):1122–6.
6. Chen S, Li L, Yu S, Zheng H, Sun Z. High dielectric constant and high-Q in microwave ceramics of $SrTiO_3$ co-doped with aluminum and niobium. J Am Ceram Soc. 2018;101(5):1835–40.
7. Zhou D, Guo D, Li WB, Pang LX, Yao X, Wang DW, et al. Novel temperature stable high-εr microwave dielectrics in the Bi_2O_3–TiO_2–V_2O_5 system. J Mater Chem C. 2016;4(23):5357–62.
8. Zhou D, Pang LX, Wang D, Li C, Jin B, Reaney IM. High permittivity and low loss microwave dielectrics suitable for 5G resonators and low temperature co-fired ceramic architecture. J Mater Chem C. 2017;5(38):10094–8.
9. Lan XK, Li J, Zou ZY, Fan GF, Lu WZ, Lei W. Lattice structure analysis and optimised microwave dielectric

properties of $LiAl_{1-x}(Zn_{0.5}Si_{0.5})_xO_2$ solid solutions. J Eur Ceram Soc. 2019;39(7):2360–4.
10. Datta R, Roy R. Phase transitions in $LiAl_5O_8$. J Am Ceram Soc. 1963;46(8):388–90.
11. Kutty T, Nayak M. Cationic distribution and its influence on the luminescent properties of Fe^{3+}-doped $LiAl_5O_8$ prepared by wet chemical methods. J Alloy Compd. 1998;269(1–2):75–87.
12. Toby BH. EXPGUI, a graphical user interface for GSAS. J Appl Crystallogr. 2001;34(2):210–3.
13. Hakki B, Coleman P. A dielectric resonator method of measuring inductive capacities in the millimeter range. IEEE T Microw Theory. 1960;8(4):402–10.
14. Shannon RD. Revised effective ionic radii and systematic studies of interatomic distances in halides and chalcogenides. Acta Crystallogr A. 1976;32(5):751–67.
15. Zhang G, Guo J, Yuan X, Wang H. Ultra-low temperature sintering and microwave dielectric properties of a novel temperature stable $Na_2Mo_2O_7$-$Na_{0.5}Bi_{0.5}MoO_4$ ceramic. J Eur Ceram Soc. 2018;38(2):813–6.
16. Yao G, Liu P, Zhang HW. Novel series of low-firing microwave dielectric ceramics: $Ca_5A_4(VO_4)_6$ (A^{2+} = Mg, Zn). J Am Ceram Soc. 2013;96(6):1691–3.
17. Fu Z, Liu P, Ma J, Zhao X, Zhang HW. Novel series of ultra-low loss microwave dielectric ceramics: $Li_2Mg_3BO_6$ (B=Ti, Sn, Zr). J Eur Ceram Soc. 2016;36(3):625–9.
18. Shannon RD. Dielectric polarizabilities of ions in oxides and fluorides. J Appl Phys. 1993;73(1):348–66.
19. Ishimaru M, Afanasyev IV, Sickafus KE. Ion-beam-induced spinel-to-rocksalt structural phase transformation in $MgAl_2O_4$. Appl Phys Lett. 2000;76(18):2556–8.
20. Dwibedi D, Murugesan C, Leskes M, Barpanda P. Role of annealing temperature on cation ordering in hydrothermally prepared zinc aluminate ($ZnAl_2O_4$) spinel. Mater Res Bull. 2018;98:219–24.
21. Li M, Pietrowski MJ, De Souza RA, Zhang H, Reaney IM, Cook SN, et al. A family of oxide ion conductors based on the ferroelectric perovskite $Na_{0.5}Bi_{0.5}TiO_3$. Nat Mater. 2014;13(1):31.
22. Zang J, Li M, Sinclair DC, Frömling T, Jo W, Rödel J. Impedance spectroscopy of $(Bi_{1/2}Na_{1/2})TiO_3$–$BaTiO_3$ based high-temperature dielectrics. J Am Ceram Soc. 2014;97(9):2825–31.
23. Rawal R, Feteira A, Flores AA, Hyatt NC, West AR, Sinclair DC, et al. Dielectric properties of the "twinned" 8H-hexagonal perovskite $Ba_8Nb_4Ti_3O_{24}$. J Am Ceram Soc. 2006;89(1):336–9.
24. Choi GK, Kim JR, Yoon SH, Hong KS. Microwave dielectric properties of scheelite and wolframite $AMoO_4$ (A=Mg, Zn, Mn) compounds. J Eur Ceram Soc. 2007;27(8–9):3063–7.
25. Bian J, Dong Y. New high Q microwave dielectric ceramics with rock salt structures: $(1-x)Li_2TiO_{3+x}MgO$ system ($0 \le x \le 0.5$). J Eur Ceram Soc. 2010;30(2):325–30.
26. Yoon SH, Kim DW, Cho SY, Hong KS. Investigation of the relations between structure and microwave dielectric properties of divalent metal tungstate compounds. J Eur Ceram Soc. 2006;26(10–11):2051–4.
27. Li J, Li C, Wei Z, Tang Y, Su C, Fang L. Microwave dielectric properties of a low-firing $Ba_2BiV_3O_{11}$ ceramic. J Am Ceram Soc. 2015;98(3):683–6.
28. Zhang J, Zuo R, Song J, Xu Y, Shi M. Low-loss and low-temperature firable $Li_2Mg_3SnO_6$-$Ba_3(VO_4)_2$ microwave dielectric ceramics for LTCC applications. Ceram Int. 2018;44(2):2606–10.
29. Ren J, Bi K, Fu X, Peng Z. Novel $Al_2Mo_3O_{12}$-based temperature-stable microwave dielectric ceramics for LTCC applications. J Mater Chem C. 2018;6(42):11465–70.
30. Yuan S, Gan L, Ning F, An S, Jiang J, Zhang T. High-$Q \times f$ $0.95MgTiO_3$–0.05 $CaTiO_3$ microwave dielectric ceramics with the addition of LiF sintered at medium temperatures. Ceram Int. 2018;44(16):20566–9.
31. Kai C, Li C, Xiang H, Tang Y, Sun Y, Fang L. Phase formation and microwave dielectric properties of $BiMVO_5$ (M = Ca, Mg) ceramics potential for low temperature co-fired ceramics application. J Am Ceram Soc. 2019;102(1):362–71.

How to cite this article: Lan X-K, Li J, Li J-P, et al. Phase evolution and microwave dielectric properties of novel $LiAl_{5-x}Zn_xO_{8-0.5x}$-based ($0 \le x \le 0.5$) ceramics. *J Am Ceram Soc*. 2019;00:1–8. https://doi.org/10.1111/jace.16791